

Constant fraction discriminator in pulsed time-of-flight laser rangefinding

Ruitong ZHENG (✉), Guanhao WU

State Key Laboratory of Precision Measurement Technology and Instruments, Department of Precision Instruments, Tsinghua University, Beijing 100084, China

© Higher Education Press and Springer-Verlag Berlin Heidelberg 2012

Abstract Constant fraction discriminator (CFD) is one of theoretic method which can locate timing point at same fraction of echo pulse in pulsed time-of-flight (TOF) laser rangefinding. In this paper, the theory of CFD method was analyzed in reality condition. The design, simulation and printed-circuit-board (PCB) performance of CFD circuit were shown. Finally, an over amplified method was introduced, by which the influence of direct-current (DC) bias error could be reduced. The experimental results showed that timing discriminator could set the timing point to a certain point on echo pulse, which did not depend on the amplitude of echo pulse.

Keywords constant fraction discriminator (CFD), time-of-flight (TOF), pulsed TOF laser rangefinding, direct-current (DC) bias error

1 Introduction

Compared with conventional laser ranging technique based on measuring the phase shift of echo pulse and start pulse, pulsed laser ranging based on time-of-flight (TOF) method can achieve longer distance and higher measurement rate [1,2]. With a scanning mirror [3] or using avalanche photodiode (APD) array as a detector, the pulsed laser range finder could scan a target and get the distance image of the target [4–6]. This technique is widely known as light detection and ranging (LiDAR). LiDAR as a novel active detection technology has been widely applied in fields such as, topographic mapping, marine surveying, atmospheric sounding, three-dimensional reality, robot vision, vehicle navigation, space science, and so on [7].

The main challenge for pulsed TOF laser rangefinding is how to accurately measure the time difference of laser pulses in sub nanoseconds (1 ns in time difference approximately equivalent to 15 cm in length). By using the Time-to-Digital IC TDC-GP2, the time can be easily measured with resolution as high as 65 ps. However, the amplitude of the echo pulse depends on the surface property of the target and the interval distance between target and LiDAR receiver. This variety of amplitude causes the walk error when measuring the time difference. Some researchers have reported their methods to decide the timing point. Palojärvi [8] carefully compared constant fraction discriminator (CFD), leading edge discriminator and high-pass timing discriminator. In this study, pulsed TOF laser rangefinding system was introduced, and the echo pulse with width approximates 7 ns, of which the rise time is only about 3 ns. So, the CFD method is more appropriate for our application. This paper was mainly about the design, simulation and experiments on the CFD circuit.

2 CFD theory

The core idea of CFD [9] is to locate the timing point at the cross point of attenuated input signal and delayed input signal shown as Fig. 1(a). By doing this, the CFD can locate the timing point on a constant fraction of the input signal. Then, the timing point is insensitive to the amplitude of the echo pulse. The theory of CFD method could be simply explained by Fig. 1(b).

The input signal of the CFD circuit could be expressed as

$$V(t) = V_0 f_0(t), \quad (1)$$

where, V_0 is the amplitude of the input signal, f_0 is the normalized function of input time varies signal.

In the CFD method, the voltage of the timing threshold $V(t_T)$ should always be

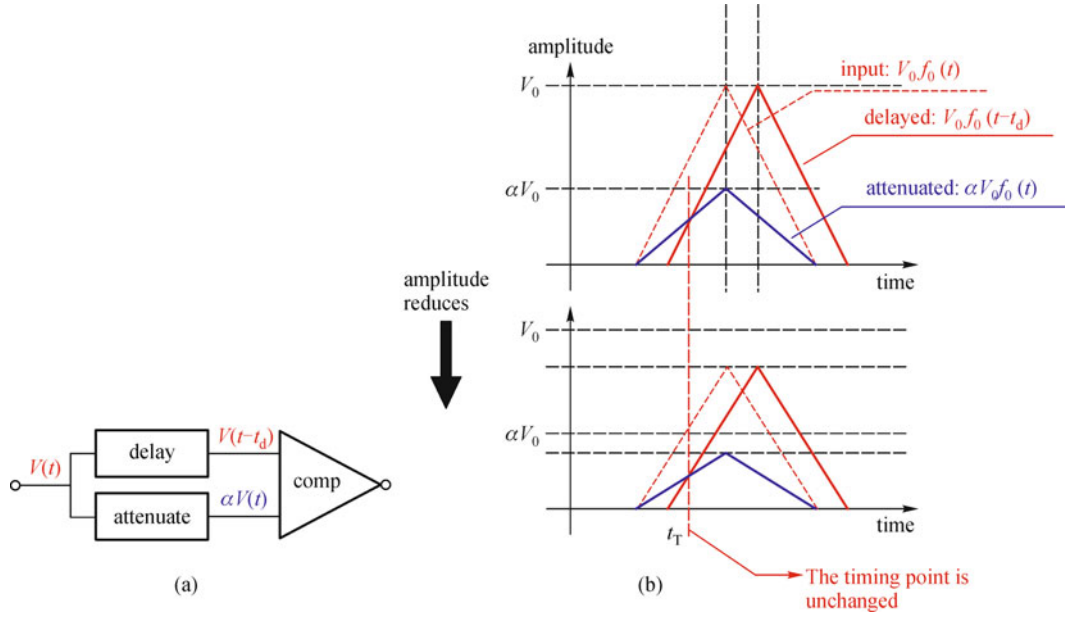


Fig. 1 Theory of CFD, triangle represents pulse shape

$$V(t_T) = pV_0, \quad (2)$$

where p is triggering ratio, a constant. From Eqs. (1) and (2), we can get that the timing point t_T , and it should satisfy the relationship

$$V_0 f_0(t_T) = pV_0. \quad (3)$$

From Eq. (3), when the shape of the input signal $f_0(t)$ is unchanged, the timing point has no relationship with the amplitude, and the timing point will be at the constant fraction of the input signal.

Setting the input signal as $V(t)$, the delayed signal could be expressed as $V(t-t_d)$, and the attenuated signal could be expressed as $\alpha V(t)$. At the timing point t_T , these two signals would intersect with each other. That is

$$V_0 f_0(t_T - t_d) = \alpha V_0 f_0(t_T). \quad (4)$$

From Eq. (4), the timing point t_T is decided by the delay time t_d and the attenuation ratio α , but it has no relationship with amplitude of input signal.

Based on Eqs. (3) and (4), the triggering ratio can be expressed as

$$p = \frac{V_{t_T}}{V_0} = \frac{V_0 f_0(t_T)}{V_0} = \frac{f_0(t_T - t_d)}{\alpha}. \quad (5)$$

That is, the triggering ratio is only influenced by the delay time t_d and the attenuation ratio α .

However, in fact there always has noise on the input signal of comparator. To avoid fake triggering of the comparator, we have to add a direct-current (DC) bias onto the attenuated signal. In this way, Eq. (4) should be changed to

$$V_0 f_0(t_T - t_d) = \alpha V_0 f_0(t_T) + V_{DC}, \quad (6)$$

where V_{DC} is the DC bias voltage on attenuated input for comparator. Accordingly, Eq. (5) should be changed to

$$p = \frac{f_0(t_T - t_d) - \frac{V_{DC}}{V_0}}{\alpha}. \quad (7)$$

Obviously, in this condition, triggering ratio depends on the amplitude (V_0) of CFD input signal. The requirement for CFD is broken. And, the DC bias V_{DC} should be as small as possible to reduce its influence on accuracy of locating the timing point.

3 Design and analysis of CFD circuit

Pulse delay circuit is illustrated in dash box of Fig. 2. The overall delay t_{GD} through the circuit can be estimated by $t_{GD} = nRC$, where n is the number of cascaded stages. Pulse attenuation could be easily achieved by resistor divider. Comparator is used to locate the timing point at the intersection of the attenuated and the delayed pulse. The circuit CFD is shown in Fig. 2.

CFD circuit with a DC bias on attenuated signal is simulated in PSpice (in Cadence 16.3). By comparison of Figs. 3 (a) and 3(b), when the amplitude of the input signal is larger (1.60 V), the timing point difference is smaller. That is, the influence of DC bias on attenuated signal to timing point accuracy is less sensitive under the condition of larger input signal. It is also obviously observed that the timing point change for red curve is less than that for blue curve. Therefore, the smaller DC bias voltage has less influence on the timing point error.

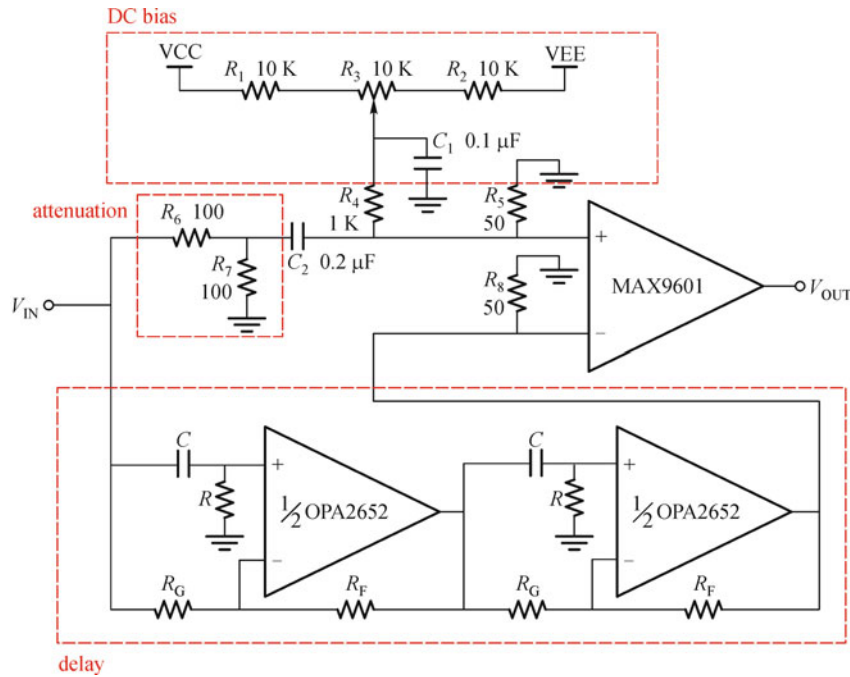


Fig. 2 CFD circuit

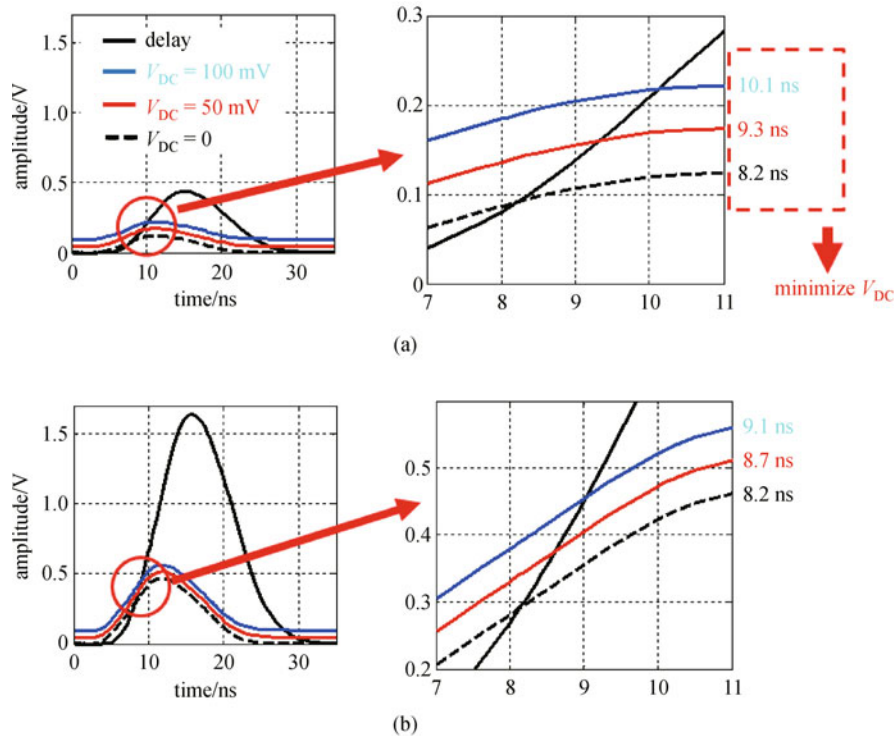


Fig. 3 Results of CFD simulation. Input signal with amplitude 0.42 and 1.60 V are shown in (a) and (b) respectively. Dash curve is delayed signal, blue curve is the attenuated signal with 100 mV DC bias and red curve is the attenuated signal with 50 mV DC bias

4 Experimental result analysis

A printed-circuit-board (PCB) was made to test the performance of the CFD circuit. The input signal is the

output of APD receiver in the laser range finder system we made before [10]. The amplitude of input signal was changed by changing the distance between the target and the ADP receiver. The waveforms of delayed and

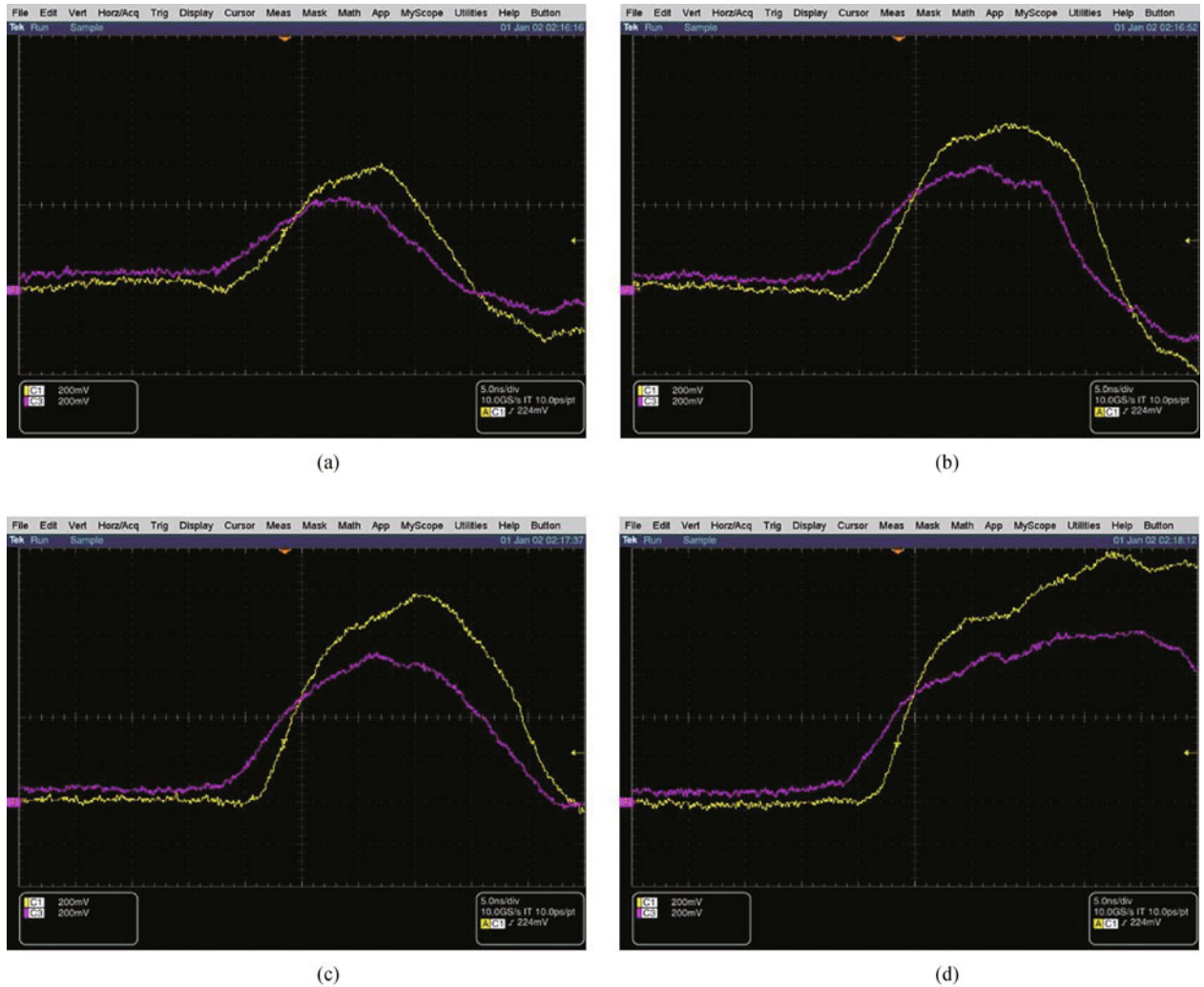


Fig. 4 Experimental result of CFD circuit. Yellow (CH1) curve is the waveform of the output of pulse delay circuit. Pink (CH3) curve is the waveform of the attenuated pulse. In sub-figures (a), (b), (c) and (d), the amplitude of pulse is 0.6, 0.8, 1.0 and 1.2 V respectively. The trigger source of the oscilloscope is set to CH1 which is the delayed signal. The trigger voltage is automatically set to 224 mV for all of the four conditions. This setup ensures the time reference keeps unchanged during the input signal increases from 0.6 to 1.2 V

attenuated signal are shown in Fig. 4. From Fig. 4, it is not difficult to find that the intersection between delayed and attenuated signals was kept fairly stable during the increasing of amplitude of the input signal from 0.6 to 1.2 V. However, we can also find that a timing point shift is about 0.5 ns in Fig. 4(a). This error may be caused by the influence of the DC bias on attenuated pulse.

There are mainly two solutions for this disadvantage in CFD circuit. One is to minimize the noise on the input signal. If the noise is small enough, the DC bias on attenuated pulse can be set to a rather small scale. However, the noise could not be reduced easily. The other possible solution is to amplify the input signal with large gain. Since the rising edge of the input signal is used in CFD, the pulse width change could be ignored. In this way, the input signal can be even amplified in saturated

mode. In Fig. 4(d), the phenomenon of saturated amplification can be already found, and the pulse was expanded obviously in Fig. 4(d).

5 Conclusions

In this paper, the theory of conventional CFD circuit was described and the influence of DC bias was analyzed in practical. Based on the simulation result and the experimental result of CFD circuit for the laser range finder, we found that the over amplify method introduced in this study to reduce the influence of DC bias, and only if the gain of amplifier linked in laser range finder is higher enough, the CFD circuit can achieve its theoretical performance.

Acknowledgements This work was sponsored by the National Natural Science Foundation of China (Grant No. 40801123).

References

1. Wang J Y, Hong G L. Technologies and applications of laser active remote sensing. *Laser & Infrared*. 2006(S1): 742–748 (in Chinese)
2. Li M, Song Y, Yu J, Li C L, Tang D. High precision laser pulse distance measuring technology. *Infrared and Laser Engineering*, 2011, 40(8): 1469–1473 (in Chinese)
3. Aloysius W, Uwe L. Airborne laser scanning—an introduction and overview. *ISPRS Journal of Photogrammetry & Remote Sensing*, 1999, 54(2–3): 68–82
4. JIANG Y B. Array imaging three dimensional lidar. Dissertation for the Doctoral Degree. Hangzhou: Zhejiang University, 2009 (in Chinese)
5. Ailisto H, Heikkinen V, Mitikka R, Myllylä R, Kostamovaara J, Mäntyniemi A, Koskinen M. Scannerless imaging pulsed-laser range finding. *Journal of Optics A: Pure and Applied Optics*, 2002, 4(6): S337–S346
6. Heinrichs R M, Aull B F, Marino R M, Fouche D G, McIntosh A K, Zayhowski J J, Stephens T, O'Brien M E, Albota M A. Three-dimensional laser radar with APD arrays. *Laser Radar Technology and Applications VI*, 2001, 4377(1): 106–117
7. Liu X B, Li L. Design of the optical system of flash lidar based on an APD array. *Infrared and Laser Engineering*, 2009, 38(5): 893–896 (in Chinese)
8. Palojärvi P. *Integrated Electronic and Optoelectronic Circuits and Devices for Pulsed Time-of-Flight Laser Rangefinding*. Finland: Oulun Yliopisto, 2003
9. HU C S. Investigation into the high-speed pulsed laser diode 3D-imaging lidar. Dissertation for the Doctoral Degree. Changsha: National University of Defense Technology, 2005 (in Chinese)
10. Zheng R, Wu G. Infrared pulsed semiconductor laser range finder. *Infrared and Laser Engineering*, 2010, 39(S): 134–138 (in Chinese)